J. Fluid Mech. (2007), *vol.* 591, *pp.* 97–116.
doi:10.1017/S0022112007007732 Printed in the United Kingdom

Contaminants in ventilated filling boxes

D. T. BOLSTER AND P. F. LINDEN

Department of Mechanical and Aerospace Engineering, University of California San Diego, La Jolla, CA 92037, USA
dbolster@uscd.edu

(Received 23 October 2006 and in revised form 28 May 2007)

While energy efficiency is important, the adoption of energy-efficient ventilation systems still requires the provision of acceptable indoor air quality. Many low-energy systems, such as displacement or natural ventilation, rely on temperature stratification within the interior environment, always extracting the warmest air from the top of the room. Understanding buoyancy-driven convection in a confined ventilated space is key to understanding the flow that develops with many of these modern low-energy ventilation schemes. In this work we study the transport of an initially uniformly distributed passive contaminant in a displacement-ventilated space. Representing a heat source as an ideal sourced of buoyancy, analytical and numerical models are developed that allow us to compare the average efficiency of contaminant removal between traditional mixing and modern low-energy systems. A set of small-scale analogue laboratory experiments was also conducted to further validate our analytical and numerical solutions.

We find that on average traditional and low-energy ventilation methods are similar with regard to pollutant flushing efficiency. This is because the concentration being extracted from the system at any given time is approximately the same for both systems. However, very different vertical concentration gradients exist. For the low-energy system, a peak in contaminant concentration occurs at the temperature interface that is established within the space. This interface is typically designed to sit at some intermediate height in the space. Since this peak does not coincide with the extraction point, displacement ventilation does not offer the same benefits for pollutant flushing as it does for buoyancy removal.

1. Introduction

People spend substantial amounts of time indoors, in many cases up to as much as 90% (Jenkins *et al.* 1992), and therefore it is important to understand the details of the the indoor environment, in particular regarding human comfort, indoor air quality (IAQ) and energy consumption. The US Energy Information Administration states that approximately 10% of the total energy consumption in the USA is consumed by heating, cooling and ventilation of buildings. Currently, the USA is the largest per capita consumer of energy in the world, but long-term forecasts to 2025 project the strongest growth in energy use will come from developing countries, especially China and India, where buoyant economies will boost demand. Furthermore the US Energy Information Administration states that energy use in developing countries is forecast to soar by 91% over the next two decades, while industrialized nations are expected to increase energy consumption by about one third. Therefore, it is important to try and reduce this growth in consumption and the consequent increase

in carbon emissions by designing better and more efficient ventilation strategies within buildings.

The adoption of energy-efficient ventilation systems requires that they also provide an acceptable level of IAQ and comfort. In order to reduce energy consumption various low-energy systems such as displacement ventilation, underfloor air distribution, operable windows, night cooling, radiant and evaporative cooling are under consideration. All these systems have the potential of 'free cooling'. That is, under certain conditions, outside air is used to cool the building and reduce the load on mechanical systems. The introduction of outside air, either through filters or simply by opening a window introduces outside pollutants. Additionally, internal pollutants are generated and need to be extracted from the building.

The many types of airborne contaminants in buildings can be put very broadly into two categories – gaseous and particulate. In this paper we focus our attention on the gaseous kind, with future work considering particulate contaminants. Gaseous contaminants are usually considered as passive contaminants that are assumed to follow exactly the air currents in a space. Some of the more common gaseous contaminants that cause concern in buildings are carbon monoxide, carbon dioxide, nitrogen oxides, ozone, sulfur dioxide, moisture, formaldehyde, radon gas and its progeny. Many of these contaminants are combustion by-products; given the proliferation of transportation and industrial sources, there is increasing concern about the levels of these contaminants in outdoor and, consequently, indoor air. Many gas-phase contaminants have obvious adverse effects on a person's health, comfort and ability to work above threshold concentrations, and teratogenic contaminants are of concern at any concentration level.

Traditional ventilation, such as that provided by a conventional overhead HVAC system, is mixing ventilation, where incoming air is mixed with the air in the room and diluted. This typically results in a relatively uniform interior temperature and contaminant distribution. In contrast, in order to benefit from free cooling, many modern low-energy ventilation schemes require the use of temperature stratification in a space, with a bottom layer of cooler comfortable air where occupants are located, and an upper layer that is comparatively warm and uncomfortable (Linden 1999). The ability to extract air at elevated temperatures is necessary for energy efficiency and free cooling. High-temperature extraction can be achieved, for example, by displacement ventilation or underfloor air distribution, where cool air enters the space at floor level and the warm air is extracted at the ceiling. Hence, stratification is an important feature in modern ventilation design. This is particularly true for tall spaces, where vertical temperature differences can be quite significant.

Many heat sources within a building (people, electronic equipment etc.) can be regarded as localized, and understanding the manner in which they stratify a space is critical to design-efficient ventilation schemes. These heat sources can often be modelled as pure sources of buoyancy, which give rise to turbulent plumes. Considerable work has examined the stratification generated by a buoyant plume within a confined space. In an unventilated space the plume produces a continuous stable stratification by the 'filling box' mechanism (Baines & Turner 1969). Warm air spreads out across the top of the space and then descends into the interior around the plume. At the later times the plume entrains this warm air, thereby continuously increasing the temperature of the air reaching the ceiling. In the absence of heat losses, the temperature everywhere within the space will increase linearly with time.

In a ventilated enclosure a steady state is eventually reached in which the heat removed by the ventilation equals that input by the plume. When the openings are

located at high and low levels, the stratification takes the form of two layers of uniform, but different, temperatures separated by an interface. The values of the temperature and the height of the interface can be calculated for different ventilation strategies: e.g. natural ventilation (Linden, Lane-Serff & Smeed 1990; Caulfield & Woods 2002; Woods, Caulfield & Phillips 2003; Kaye & Hunt 2004) and displacement or underfloor ventilation (Lin & Linden 2002; Liu & Linden 2006; Coffey & Hunt 2007).

It is often stated that displacement ventilation systems can be more effective at removing contaminants (e.g. Lin *et al.* 2005; Xinga, Hatton & Awbi 2001; Brohus & Nielsen 1996) and practitioners use this as a strong selling point. This relies on the belief that the contaminants will be transported into the hot upper layer, where they will be extracted. However, caution must be taken as this may not be universally true. Experimental studies (Mundt 2001) have shown that the ventilation effectiveness of a displacement system can be sensitive to the location and type of the contaminant source involved.

Various CFD studies have been conducted looking at contaminant transport in displacement and similar ventilation systems (Qiu-Wang & Zhen 2006; He, Yang & Srebric 2005; Zhang & Chen 2006) on the transport of contaminants in specific building geometries. However, even with current computer speeds, full-scale simulations can be prohibitively expensive, particularly for large buildings with multiply connected spaces. Accurate CFD simulations of such flows can be very difficult, because of uncertain boundary conditions (Cook, Ji & Hunt 2003), the difficulties involved in accurately modelling thermal plumes (Yan 2007; Murakami, Ohira & Kato 2000) and the appropriate selection of a wide choice of available turbulence models (Ji, Cook & Hanby 2007), which can all affect the flows involved in a non-negligible manner.

Reduced analytical models (such as the one we present in this paper) can be useful, as they can be integrated into zonal energy simulation models (e.g. the US Department of Energy code EnergyPlus) where connected spaces are treated as nodes that communicate with one another via conservation equations (e.g. temperature, contaminant concentration etc.). Further, such analytical models provide important benchmarks, necessary for the validation of CFD models. Also, while useful for specific cases, CFD studies do not always provide practical information about the general physics and behaviour of contaminants in low-energy ventilation systems.

Few theoretical studies on contaminant transport in low-energy ventilated spaces have been conducted. Hunt & Kaye (2006) considered a pollutant flushing problem in a naturally ventilated space containing isolated sources of buoyancy. They modelled the space as two well-mixed regions. Additionally, in a follow-up paper, Kaye & Hunt (2007) considered the influence of distributed, rather than isolated, heat sources that, for an equal buoyancy input, can result in very different flow rates

In this paper we are concerned with the transport of passive contaminants in 'forced' displacement systems where cool, clean air is introduced into the lower part of a space with an initially uniform concentration of a contaminant. A theoretical model, based on plume theory and an extension of the Baines & Turner (1969) 'filling box' approach, is given in § 2. The results of this model are described in § 3. A set of experiments designed to test the model and a comparison of the results with the theoretical predictions is given in § 4. The conclusion and applications to IAQ are discussed in § 5.

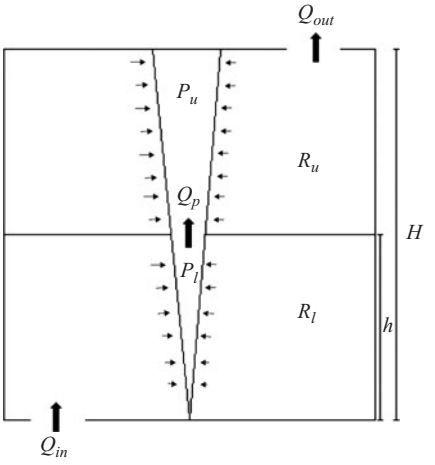

FIGURE 1. Displacement ventilation with a single ideal plume heat source. $P(z)$ is the concentration of contaminant in the plume and $R(z)$ the concentration in the room.

2. Theoretical model

Consider a space with a single ideal heat source, and inlet and extraction vents at the top and bottom of the room, respectively (figure 1). We will consider the rate of removal of a passive contaminant with uniform initial concentration C_0. The flow rates, Q_{in} through the space can be specified, as desired, either as a fixed ventilation flow supplied by a fan in a mechanical system (Sandberg & Etheridge 1996) or as determined by the strength of plume and size of openings in a naturally ventilated enclosure (Linden *et al.* 1990). The resulting stratification has two layers of uniform temperature with cool air in the lower layer (corresponding to the temperature of the air introduced through the lower vent) and warm buoyant air in the upper layer.

2.1. *Flow in space*

The flow within the space is determined by coupling the plume flow with the environment outside the plume. For a Boussinesq plume with assumed top hat profiles, in which the density differences are sufficiently small that they only affect the buoyancy force, the equations for mass, momentum and buoyancy conservation in the plume are

$$\frac{\mathrm{d}Q}{\mathrm{d}z} = 2\alpha M^{1/2}, \quad M\frac{\mathrm{d}M}{\mathrm{d}z} = FQ, \quad \frac{\mathrm{d}F}{\mathrm{d}z} = \frac{g}{\rho_0}\frac{\mathrm{d}\rho_a}{\mathrm{d}z}Q, \tag{2.1}$$

where πQ is the volume flux, πM is the specific momentum flux and πF is the specific buoyancy flux (Morton, Taylor & Turner 1956; hereafter referred to as MTT). The entrainment constant, α, defined in MTT relates the vertical velocity scale in the plume to the entrainment velocity on the edge of the plume.

In order to couple the plume to the environment we assume that the cross-sectional area A of the room is sufficiently large such that at all heights the plume occupies a negligible fraction of the area, i.e. $b \ll A$. Therefore, the entrainment into the plume should essentially be horizontal and the MTT plume equations written above can still be applied (Baines & Turner 1969). When the plume impinges on the ceiling it spreads horizontally to the sidewalls, which then cause the resulting warm air to

descend into the space. Volume conservation in the region outside the plume is

$$wA = -\pi Q - Q_{out}, \tag{2.2}$$

where $w(z)$ is the vertical velocity outside the plume and Q_{out} is the volume flow rate out of the space through the upper vent. Provided that heat conduction is negligible (i.e. the Péclet number is sufficiently high), the conservation of mass equation is

$$\frac{\partial \rho_a}{\partial t} + w\frac{\partial \rho_a}{\partial z} = 0, \tag{2.3}$$

where ρ_a is the density in the ambient fluid outside the plume. It is necessary to assume that the background density in the room varies on a much slower time scale than that associated with the evolution of the plume, which requires

$$\left(\frac{5}{6\alpha}\right)^2 \frac{A}{\pi H^2} \gg 1 \tag{2.4}$$

(Baines & Turner 1969). The restriction requires the room to have a large aspect ratio A/H^2.

The interface that divides the upper and lower layer corresponds to the height where the plume flow rate is the same as the flow rate through the vents (i.e. when $Q = Q_{in}$ or Q_{out} and where $w(z) = 0$).

2.2. *Contaminant transport*

Contaminant with concentration $R(z)$ in the room is entrained into the plume, which has contaminant concentration $P(z)$. Conservation of contaminant volume flux in the plume can be expressed as

$$\frac{\mathrm{d}}{\mathrm{d}z}[PQ] = 2\alpha M^{1/2} R, \tag{2.5}$$

and using (2.1) we obtain

$$\frac{\mathrm{d}P}{\mathrm{d}z} = \frac{2\alpha M^{1/2}(R - P)}{Q}. \tag{2.6}$$

In addition, neglecting diffusion, the room contaminant conservation equation is

$$\frac{\partial R}{\partial t} + w\frac{\partial R}{\partial z} = 0. \tag{2.7}$$

We now consider the flow in the upper and lower layers separately (see figure 1), and solve (2.1), (2.2), (2.5) and (2.6).

The lower layer

In the unstratified lower layer ($0 < z < h$), the plume buoyancy flux remains constant ($F(z) = F_0$) and the solutions for Q and M are

$$Q(z) = \frac{6\alpha}{5}\left(\frac{9\alpha F_0}{10}\right)^{1/3} z^{5/3}, \quad M(z) = \left(\frac{9\alpha F_0}{10}\right)^{2/3} z^{4/3}, \quad 0 < z < h. \tag{2.8}$$

Substituting (2.7) into (2.2) and (2.5), the contaminant transport equations for the lower layer become

$$\frac{\mathrm{d}P_l}{\mathrm{d}z} = \frac{5}{3z}(R_l - P_l), \tag{2.9}$$

where the subscript l refers to the concentrations in the lower layer and

$$w = \frac{\pi}{A}\left(\frac{6\alpha}{5}\left(\frac{9\alpha F_0}{10}\right)^{1/3}\right)(h^{5/3} - z^{5/3}), 0 < z < h. \tag{2.10}$$

The upper layer

In the upper layer ($h < z < H$) the density outside is the same as the density of the plume at the interface so that the plume is no longer buoyant above the interface ($F = 0$). The momentum flux M is constant and equal to the momentum flux of the plume at the interface (i.e. $M = M_p$). This implies

$$(z) = Q_p + 2\alpha M_p^{1/2}(z - h), \quad M_p = \left(\frac{9\alpha F_0}{10}\right)^{2/3} h^{4/3}, \quad h < z < H. \tag{2.11}$$

Therefore, the contaminant transport equations become

$$\frac{\mathrm{d}P_u}{\mathrm{d}z} = \frac{1}{z - (2/5)h}(R_u - P_u), \qquad w = \frac{\pi}{A}\left(2\alpha\left(\frac{9\alpha}{10}\right)^{1/3} F_0^{1/3} h^{2/3}\right)(h - z), h < z < H, \tag{2.12}$$

where the subscript u refers to the concentrations in the upper layer.

2.3. *Non-dimensionalization*

We non-dimensionalize the variables as follows:

$$z = \zeta H, \quad P = C_o p, \quad R = C_o r, \tag{2.13}$$

$$w = w^* \frac{\pi}{A}\frac{6\alpha}{5}\left(\frac{9\alpha}{10}F_0\right)^{1/3} h^{5/3}, \quad t = \tau\frac{AH}{Q_{in}} = \tau\frac{AH}{\pi(6\alpha/5)(9\alpha F_o/10)^{1/3}h^{5/3}}, \tag{2.14}$$

where C_0 is the initial uniform concentration of contaminant in the space.

The replenishing time, which represents the time taken for a volume of fluid equal to the volume of the space to enter that space (i.e. V_{room}/Q_{in}) is used to non-dimensionalize time. The characteristic velocity is chosen as the plume flux at the interface divided by the cross-sectional area of the room. This is the background ambient velocity that would exist in the absence of ventilation with the exterior (i.e. a pure 'filling box').

Using the above non-dimensionalization, the contaminant and velocity equations for the lower and upper layers, respectively, become

$$\frac{\mathrm{d}p_l}{\mathrm{d}\zeta} = \frac{5}{3\zeta}(r_l - p_l), \quad w_l^* = \left(1 - \left(\frac{\zeta}{\zeta_h}\right)^{5/3}\right) \tag{2.15}$$

and

$$\frac{\mathrm{d}p_u}{\mathrm{d}\zeta} = \frac{1}{\zeta - \frac{2}{5}\zeta_h}(r_u - p_u), \quad w_u^* = \frac{5}{3}\left(1 - \frac{\zeta}{\zeta_h}\right). \tag{2.16}$$

2.4. *Analytical solutions*

In practice it is often difficult to obtain a pure displacement flow in the lower layer and some mixing may occur as a result of inflow through the lower vents. Consequently, we consider two limiting cases for the lower layer: pure displacement ventilation and a well-mixed lower layer (figure 2). These cases span the extremes of inflow with no mixing and complete mixing. We do not assume that the upper layer is well mixed, but calculate the development of the flow in the upper layer using a modification of

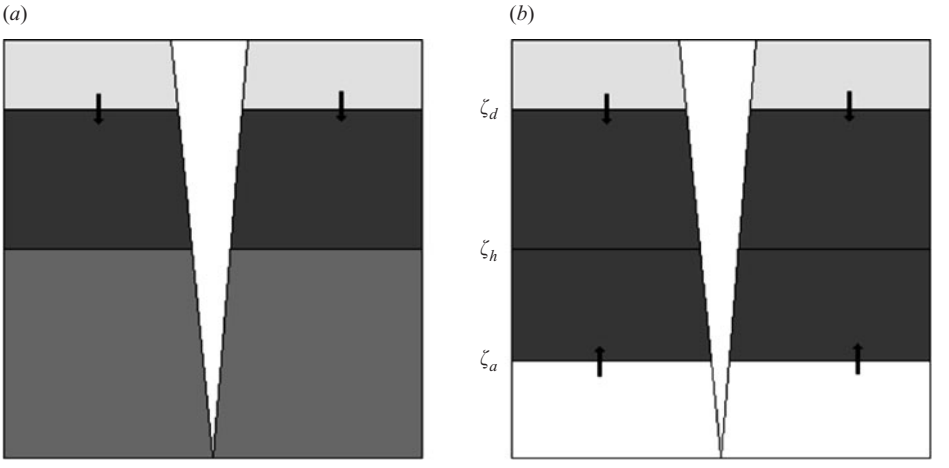

FIGURE 2. Sketch of ascending and descending fronts in the room: (*a*) corresponds to a well mixed lower layer, while (*b*) corresponds to a displaced lower layer. Darker shades imply higher contaminant concentrations.

the filling box mechanism. This is in contrast to Hunt & Kaye (2006), who considered the case where both the lower and upper layers are well mixed. While there will be some mixing in the upper layer, a well-mixed model does not capture some of the interesting dynamics which we observe in the upper layer with both our models and experiments.

2.4.1. *Well-mixed lower layer*

Let the concentration of the lower layer be denoted by c, with the initial condition $c(\tau = 0) = 1$. For the well-mixed case (figure 2*a*) the concentration in the lower layer to decay exponentially as:

$$c = \mathrm{e}^{-\tau/\zeta}. \tag{2.17}$$

Since in this case the lower layer has a uniform concentration c (figure 2*a*), the concentration of the fluid being transported by the plume into the upper layer is also of concentration c (i.e. $p_l = c$ everywhere in the lower layer). This gives us a required boundary condition for (2.14) for p_u in the upper layer.

2.4.2. *Displaced lower layer*

For the case of displacement ventilation in the lower layer there is an ascending front, which we will denote by ζ_a with fresh uncontaminated ambient fluid ($c = 0$) below it and fluid of the initial concentration ($c = 1$) above it. The lower layer is therefore now split into two distinct regions (figure 2*b*).

Since, from (2.13), the background flow velocity w_l for the lower layer is known, we can track the position of this ascending front. Its evolution is given by

$$\frac{\mathrm{d}\zeta_a}{\mathrm{d}\tau} = \left(1 - \left(\frac{\zeta_a}{\zeta_h}\right)^{5/3}\right), \tag{2.18}$$

which can be rewritten as

$$\frac{\mathrm{d}\zeta_a}{\left(1 - (\zeta_a/\zeta_h)^{5/3}\right)} = \mathrm{d}\tau. \tag{2.19}$$

We write the left-hand side as its Laurent/Frobenius series expanded about $\zeta = 0$:

$$\frac{\mathrm{d}\zeta_a}{\left(1-(\zeta_a/\zeta_h)^{5/3}\right)} = \mathrm{d}\zeta_a \sum_{n=0}^{\infty} \left(\frac{\zeta_a}{\zeta_h}\right)^{5n/3}. \tag{2.20}$$

Equation (2.18) can be integrated, and the solution to (2.17), with the initial condition at $\tau = 0$, $\zeta_a = 0$ (i.e. we are tracking the first ascending front), is

$$\sum_{n=0}^{\infty} \left(\frac{(3/(5n+3))\zeta_a^{5n+3/3}}{\zeta_h^{5(n)/3}}\right) = \tau. \tag{2.21}$$

The long time limit (as $t \to t_\infty$ and $h_a \to h$) gives

$$\tau_\infty = 3\zeta_h \sum_{n=0}^{\infty} \left(\frac{1}{5n+3}\right). \tag{2.22}$$

This series does not converge, which suggests that it takes an infinite amount of time for all the contaminant to be removed from the lower layer (in practice, of course, this contaminant layer becomes so thin as to be unimportant).

While (2.19) is a solution for the ascending front, it is difficult to determine the height of the interface at a given time owing to the nonlinearity of the equation.†

Given ζ_a, we can solve for the contaminant concentration in the plume using (2.13). Below ζ_a, $p_l = 0$ since the ambient concentration is zero. Above ζ_a, the room concentration is 1, which results in

$$\frac{\mathrm{d}p_l}{(r_l - p_l)} = \frac{5}{3}\frac{\mathrm{d}\zeta}{\zeta}, \quad p_l(z = \zeta_a) = 0. \tag{2.23}$$

This means that the plume and background concentrations in the lower layer are

$$r_l = 0, \quad p_l = 0, \quad 0 < \zeta < \zeta_a \tag{2.24}$$

and

$$r_l = 1, \quad p_l = 1 - \left(\frac{\zeta_a}{\zeta}\right)^{5/3}, \quad \zeta_a < \zeta < \zeta_h. \tag{2.25}$$

2.4.3. *The upper layer*

Using w_u^* (2.14), the interface equation for the upper layer is

$$\frac{\mathrm{d}\zeta}{\mathrm{d}\tau} = w_u^* = \frac{5}{3}\left(1 - \frac{\zeta}{\zeta_h}\right). \tag{2.26}$$

Integrating and using the boundary condition that, at time $\tau = \tau'$, $\zeta = 1$ (this is how τ' is defined), we get

$$\zeta = \zeta_h + (1 - \zeta_h)\mathrm{e}^{(-5(\tau-\tau'))/(3\zeta_h)}. \tag{2.27}$$

Define $\tau' = 0$ as the starting time, which marks the 'first descending front', ζ_d. In the same manner as for the displaced lower layer there will be a region, which will remain

† The sum in the equation for h_a, (2.21), can be expressed as the following tabulated function, which might make it easier to find the solution within a numerical iterative scheme:

$$\sum_{n=0}^{\infty} \left(\frac{(3/(5n+3))h_a^{(5n+3)/3}}{h^{5(n+1)/3}}\right) = \frac{3h_a}{5h^{5/3}} \quad \mathrm{LerchPhi}\left(\frac{h_a^{5/3}}{h^{5/3}}, 1, 1, \frac{3}{5}\right).$$

at the initial concentration, below this first front. The front will migrate downwards as:

$$\zeta_d = \zeta_h + (1 - \zeta_h)\mathrm{e}^{-5/(3\tau\zeta_h)}. \tag{2.28}$$

We therefore have two regions in the upper layer of the space: a lower part, below the descending front ($\zeta_h < \zeta < \zeta_d$), where the concentration is 1, and an uppermost layer ($\zeta_d < \zeta < 1$), where the concentration is changing over time.

Below the descending front

Below the descending front $r = 1$, so the concentration in the plume, subject to the boundary condition that p is continuous across the interface (i.e. $p_l(\zeta = \zeta_h)$ in the upper layer is $p_u(\zeta = \zeta_h)$ from our lower-layer equations), is

$$r = 1, \quad p = 1 - \frac{3(1 - p(\zeta_h))\zeta_h}{5\zeta - 2\zeta_h}, \quad \zeta_h < \zeta < \zeta_d. \tag{2.29}$$

Above the descending front

This region is more difficult to model, because the background concentration r changes over time and is not constant with height. From (2.24), for the upper layer we know that r is constant along the position defined by

$$\zeta = \zeta_h + (1 - \zeta_h)\mathrm{e}^{5(\tau - \tau')/(3\zeta_h)}, \tag{2.30}$$

where τ' is the time when this concentration front is at the top of the chamber,

$$\tau' = \tau - \frac{3\zeta_h}{5}\ln\left(\frac{\zeta - \zeta_h}{1 - \zeta_h}\right). \tag{2.31}$$

Therefore, at some height ζ and time τ, the background concentration $r(\zeta, \tau)$ is the same as the background concentration $r(1, \tau')$ at the top of the room, which, in turn, is the concentration in the plume at the top of the room at time τ', i.e.

$$r(\zeta, \tau) = r(1, \tau') = p(1, \tau'). \tag{2.32}$$

Hence the plume concentration equation can be written as

$$\frac{\mathrm{d}p}{\mathrm{d}\zeta} = \frac{p(\zeta = 1, \tau = \tau - (3\zeta_h/5)\ln((\zeta - \zeta_h)/(1 - \zeta_h)) - p(\zeta, \tau)}{\zeta - (2/5)\zeta_h}, \tag{2.33}$$

which has the general solution

$$p(\zeta) = \frac{5\displaystyle\int_{\zeta_d}^{\zeta} r(\zeta')\,\mathrm{d}\zeta' + p(\zeta_d)(5\zeta_d - 2\zeta_h)}{5\zeta - 2\zeta_h}, \quad r(\zeta, \tau) = p(1, \tau'). \tag{2.34}$$

Consider the integral form of conservation equation for the contaminant in the region above the descending front

$$\frac{\mathrm{d}}{\mathrm{d}t}\left(\int_{\zeta_d}^{1} r\,\mathrm{d}\zeta\right) = q(\zeta = \zeta_d)p(\zeta = \zeta_d) - q_{out}r(\zeta = 1). \tag{2.35}$$

Noting that $r(1, \tau) = p(1, \tau)$ and defining $r^* = \displaystyle\int_{\zeta_d}^{1} r\,\mathrm{d}\zeta$, (2.35) can be written as

$$\frac{\mathrm{d}r^*}{\mathrm{d}\tau} = f(\tau) - c_1 r^*, \tag{2.36}$$

where

$$f(\tau) = p(\zeta_d)\left(\frac{5(1-\zeta_d)}{5-2\zeta} + \frac{5(\zeta_d-\zeta)}{3\zeta}\right), \quad c_1 = \frac{5}{5-2\zeta}. \tag{2.37}$$

The general solution to (2.34) and (2.35) is

$$r^* = \frac{\int (\mathrm{e}^{c_1\tau} f(\tau))\mathrm{d}\tau + D}{\mathrm{e}^{c_1\tau}}. \tag{2.38}$$

For the well-mixed lower-layer case the solution is

$$r^* = C_1 \exp\left(\frac{5\tau}{2\zeta-5}\right) - \frac{\zeta-1}{7\zeta-5}\left(5\zeta\exp\left(\frac{-\tau(7\zeta-5)}{\zeta(2\zeta-5)}\right) - 7\zeta\exp\left(\frac{-25\tau(\zeta-1)}{3\zeta(2\zeta-5)}\right) + 5\exp\left(\frac{-25\tau(\zeta-1)}{3\zeta(2\zeta-5)}\right)\right)\exp\left(\frac{5\tau}{2\zeta-5}\right), \tag{2.39}$$

where, for the initial condition $r^*(\tau=0)=0$,

$$C_1 = \frac{(\zeta-1)(5-2\zeta)}{7\zeta-5}. \tag{2.40}$$

Unfortunately, owing to the difficulty in solving (2.18), we cannot find an analytic solution for the displaced lower-layer case. Instead we integrate (2.16) and (2.33) numerically and present the semi-analytical results.

Figure 3 shows the average concentration within the space for the three cases, an entirely well-mixed room, a well-mixed lower layer, and a displaced lower layer, for three values for the interface height, $\zeta_h = 0.2$, 0.5 and 0.8. We present the entirely well-mixed room case, first because it allows us to compare the efficiency of contaminant removal of a displacement ventilation system with that of a traditional mixing system. Second, it allows us to discuss the validity of the 'well-mixed' assumption. This assumption is typically used in building simulations, which treat each room as a well-mixed space that communicates with its neighbouring spaces via integral conservation laws. It is widely believed that this assumption is probably not a good one for displacement-ventilated spaces owing to the vertical non-uniformity.

The first and probably most surprising thing to note from figure 3 is that the well-mixed assumption matches the other models in accounting for the global amount of contaminant within the room. Figure 3(*d*)–(*f*) shows that the differences are small. The differences become larger between ideal displacement and the fully mixed model as the interface height increases. Therefore, this suggests that displacement ventilation only offers a small benefit in removing a contaminant over mixing ventilation, in terms of the total amount of contaminant in the room.

2.5. *Comparison with Hunt & Kaye* (2006)

In this section we compare the results of this paper with those of Hunt & Kaye (2006), who assumed perfect mixing in both the upper and lower layers. Since the average concentrations are approximately the same (figure 3), we only compare the model where we assume a well-mixed lower layer. The concentration in the lower layer is given by (2.17). We therefore define the decay rate of the lower layer as $\phi_{low} = 1/\zeta$, which is identical to the decay rate of the lower layer in Hunt & Kaye (2006) (when rewritten with the current non-dimensionalization). This should be obvious since the mechanism for pollutant removal from the lower layer is identical for our well-mixed model and that of Hunt & Kaye (2006). Therefore, any differences between the models

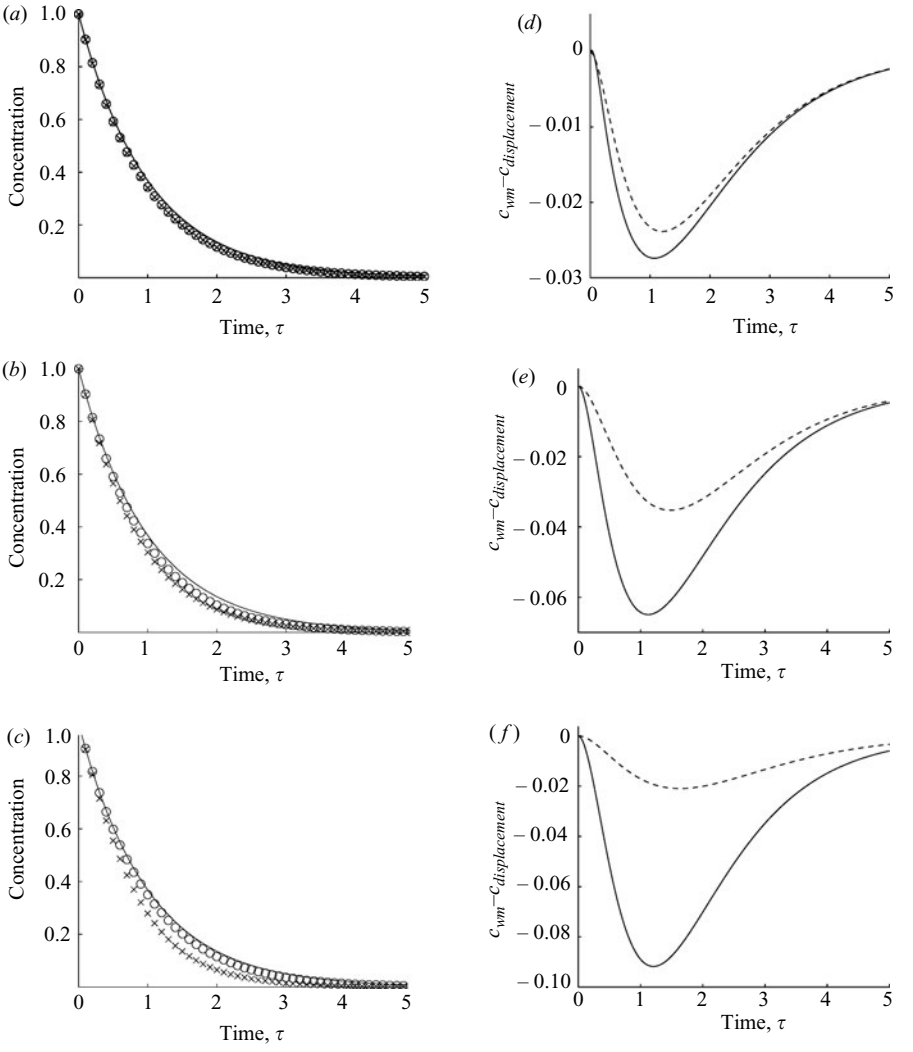

FIGURE 3. Comparison of concentrations averaged over the whole height of the box. (*a*)–(*c*) Average concentration for each of the three models, well-mixed entire (–), well-mixed lower layer (○), displaced lower layer (×), versus time for $\zeta_h = 0.2$ (*a*), 0.5 (*b*) and 0.8 (*c*). (*d*)–(*f*) The difference in average concentration between the two layer models and the well-mixed model; well-mixed lower layer (- -), displaced lower layer (–).

can only occur in the upper layer. The average concentration of the upper layer is given by

$$\bar{c}_u = \frac{1}{1-\zeta}((\zeta_d - \zeta_h) + r^*), \tag{2.41}$$

which can be written as

$$\bar{c}_u = \frac{1}{7\zeta - 5}\left((2\zeta - 5)\mathrm{e}^{-5\tau/(5-2\zeta)} + 5\zeta\,\mathrm{e}^{(-\tau/\zeta)}\right). \tag{2.42}$$

Following Hunt & Kaye (2006), we define the upper layer decay rate as $\phi_{up} = (5/5 - 2\zeta)$. This is different from that of Hunt & Kaye (2006), which is

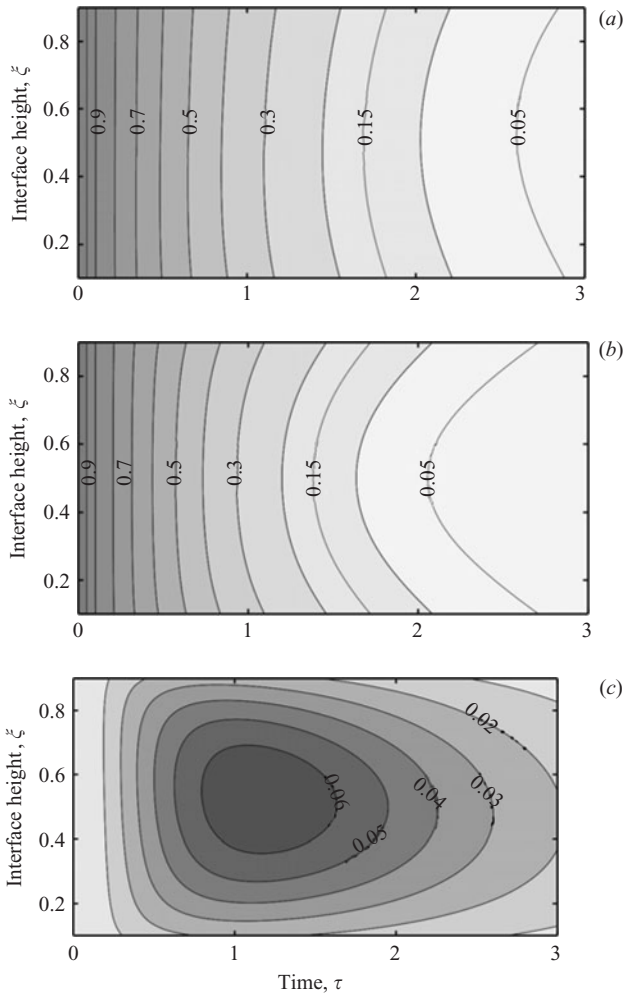

FIGURE 4. Isocontour plot of the average concentration across the entire box for time against interface height: (*a*) our solution (well-mixed lower layer), (*b*) Hunt & Kaye (2006), (*c*) the difference between (*a*) and (*b*).

$\phi_{up}^{HK} = 1/(1-\zeta)$ (again converted to the current non-dimenzionalization). It can readily be seen that $\phi_{up} < \phi_{up}^{HK}$ for all values of ζ, which suggests that the upper layer flushes pollutant out more quickly in the Hunt & Kaye model than the present one. Therefore, we expect the Hunt & Kaye (2006) model to remove contaminant more quickly, which is precisely what is observed and discussed below.

Combining the lower- and upper-layer concentrations, the average concentration in the entire box is given by

$$\bar{c} = \frac{(-2\zeta^2 + 7\zeta - 5)\mathrm{e}^{-5\tau/(5-2\zeta)} + 2\zeta^2 \mathrm{e}^{-\tau/\zeta}}{7\zeta - 5}. \tag{2.43}$$

Figure 4 depicts isocontours of concentration across a wide range of interface heights ($0.1 < \zeta < 0.9$) against time for (*a*) the well-mixed lower-layer model, (*b*) the model of Hunt & Kaye (2006), and (*c*) the difference between these two. The plots displayed in figure 3 are cross-sectional cuts of these isocontours for $\zeta = 0.2, 0.5, 0.8$.

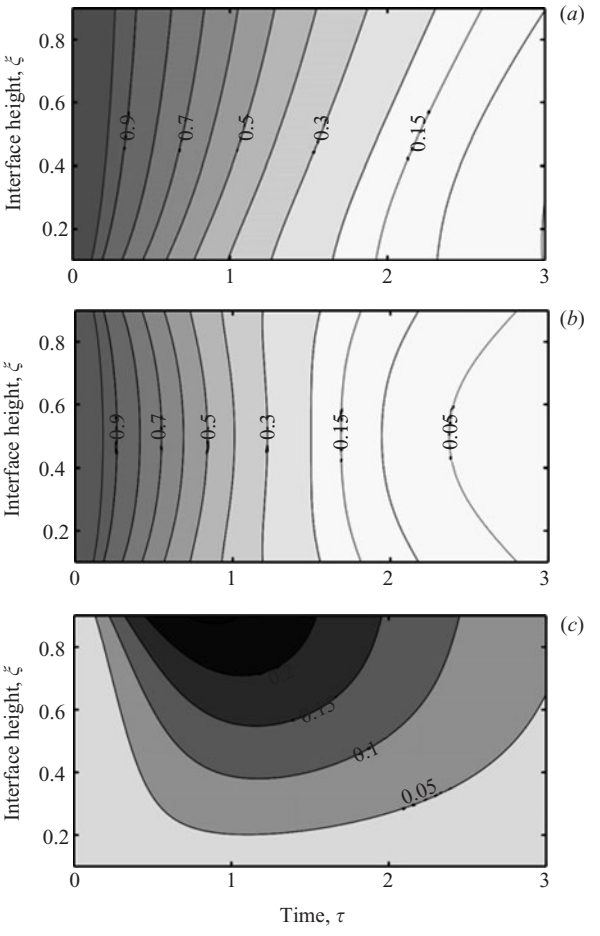

FIGURE 5. Isocontour plot of the average concentration in the upper layer against time for a full range of interface heights: (*a*) our solution (well-mixed lower layer), (*b*) Hunt & Kaye (2006), (*c*) the difference between (*a*) and (*b*).

Qualitatively the models behave similarly, with the most rapid decay corresponding to values of $\zeta = 0.5$ in both cases. This value of ζ also acts as a line of up/down quasi-symmetry (i.e. the average concentration for $\zeta = 0.5 + x'$ is the approximately the same as that for $\zeta = 0.5 - x'$). It is a line of exact symmetry for Hunt & Kaye's model. However, it is only approximately true for our model. Quantitatively, there is some disagreement. The average concentrations predicted by Hunt & Kaye's model are always smaller than those of our model as illustrated in figure 4(*c*). The peak differences occur just after $\tau = 1$ for interfaces close to the middle of the room, and then become smaller at later times. This quantitative disagreement may not appear too significant with the maximum values corresponding to 6% of the initial concentration. However, these differences can be as large as 33% when compared with each other.

Since the concentration in the lower layer is identical for our model and that of Hunt & Kaye (2006), any differences that are observed can only be attributed to the concentration in the upper layer. Figure 5 displays equivalent isocontours to those of figure 4, but only for the upper-layer average concentration. Unlike the plots of figure 4, the results predicted by the two models differ both qualitatively and

quantitatively. There is still an up/down symmetry for Hunt & Kaye's model, but this symmetry is broken in the present model, with the concentrations in the upper layer increasing monotonically with interface height. The quantitative differences between the models is also large and increases with higher values of ζ, peaking close to $\tau = 1$ at a value of 0.25. Recall, though, that such large differences were not observed when considering the average quantity of contaminant in the whole box. This is because, while the largest differences in upper-layer concentration occur for higher values of ζ, this also implies that the weighted effect (i.e. $\bar{c}_{up}(1-\zeta)$) on the total average contaminant is smaller.

In order to understand why these differences in the average concentration of the upper layer occur, it is essential to understand the vertical distribution of contaminant within the upper layer. This is discussed in detail in § 3.

3. Numerical method

The analytical solution provides sufficient information to calculate the total amount of contaminant and provides an approximate description of the contaminant distribution within the space. However, the detailed structure of the upper layer above the descending front is not resolved, and in order to determine the vertical concentration profile we solve the system of equations using a modification of a numerical scheme originally developed by Germeles (1975).

In this scheme the background ambient fluid is discretized into a finite number of layers, n, and it is assumed that the plume evolves on a faster time scale than the ambient (see (2.4) for details). Therefore, for any given time step, the equations associated with the plume are solved assuming that the background does not vary. The equations can be solved through the entire height of the room using a Runge–Kutta scheme.

Once the plume equations have been solved, the background layers, whose concentration and density remain unchanged during a particular time step, are advected with a velocity computed from (2.2). This process captures the entrainment of fluid from each layer by the rising plume since the advected layers reduce in thickness at each time step. When the plume reaches the ceiling a new layer is added, the thickness of which is determined by the flow rate of the plume at the top of the room and size of the chosen time step. The contaminant concentration assigned to this new layer is the same as the concentration of contaminant in the plume at the top of the room.

Figure 6 displays the vertical concentration profiles computed with the Germeles algorithm for an interface height corresponding to half the height of the room. Both displaced and well-mixed lower-layer cases are considered. For the sake of comparison the case of an entirely well-mixed room (vertical dashed line) is also shown. In the previous section we showed that the average reduction of contaminant is approximately the same for all three cases. Here, however, we see that the vertical distribution of contaminant is very different for displacement and mixing ventilation.

The concentration at the top of the room for all three models is approximately the same at all times. Therefore, the concentration of contaminant being extracted is about the same in all cases, which is why the reduction in average concentration does not vary significantly between the three systems. On the other hand, the 'occupied' lower-layer concentration is always less in both two-layer models than in the entirely well-mixed case, which is clearly desirable. However, the concentration of contaminant in the upper layer is always higher. Further, the peak in contaminant concentration

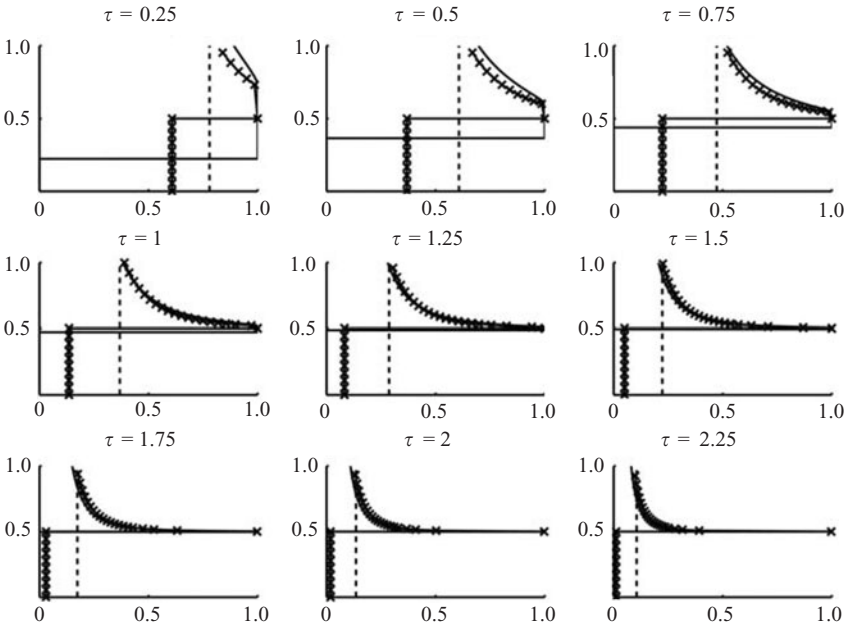

FIGURE 6. Comparison of concentration profiles at intervals of 0.25τ for $\zeta_h = 0.5$ for an entirely well-mixed space (- -), a well mixed lower layer (×—) and a displaced lower layer (–).

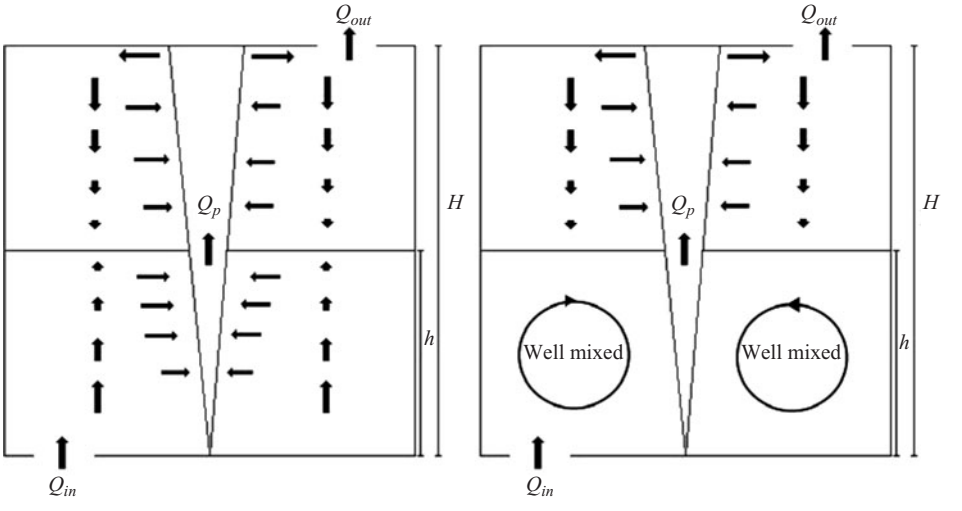

FIGURE 7. Background velocity fields for the displaced and well mixed lower-layer cases.

is always located at and just above the height of the interface. This stems from the background velocity field: see figure 7. In the upper layer the flow is all downward, while in the lower layer it is upward or mixed. The interface dividing the upper and lower layers corresponds to the height where the background velocity is zero. Therefore, the high initial concentration in the upper layer is continuously being pushed down towards the interface, causing the peak level to occur there.

4. Experiments

A series of analogue laboratory experiments, based on the salt bath technique (Linden 1999) was conducted to compare with the predictions of the theoretical models. The space is represented by a Plexiglas tank ($30 \times 30 \times 40$ cm), within which there is a low-momentum plume source (Hunt, Cooper & Linden 2000). There are openings on the lower and upper surfaces through which we pump and extract water. The plume source is located at the top centre of the tank and injects negatively buoyant (heavier) salt water. The geometry is inverted compared to the model described in the previous sections. Owing to the Boussinesq behaviour of the system this inversion has no effect on the dynamics. Fresh water is pumped in through the upper openings using an aquarium pump connected to a reservoir of fresh water. The saltier water (equivalent to the warmer air in our model) is extracted from the lower vents. By adjusting the flow rate into the tank we can adjust the interface height for a given value of source buoyancy flux.

The densities of the injected salt water for the plume ranged between 0.5% and 2% greater than that of fresh water (i.e. 1003–1018 kg m^{-3}). The flow rates through the plume nozzle were between 0.4 and 2 ml s^{-1}, resulting in source buoyancy fluxes that can vary between 2×10^{-8} and 4×10^{-7} m^4 s^{-3}. The fresh-water ventilation flow rate into the tank was varied between 0.01 and 0.15 l s^{-1} in order to adjust the height of the interface to the desired value.

In order to achieve ideal displacement it is desirable to have fluid with the least-possible momentum entering the space in order to minimize mixing in the upper (lower in model) layer. However, owing to space restrictions, which also occur in real buildings, there is a limit to how much area can be dedicated to inlet vents. In our experiments there are twelve 2.5-cm-diameter holes spread across the top of the Plexiglas tank, which act as inlet vents. Further, in order to reduce the momentum of the incoming fluid, horizontal struts, 5 cm wide, are placed 2.5 cm below the inlet holes. These reduce the momentum and deflect the incoming flow horizontally.

Two reservoirs of fresh-water supply the tank. One is 'contaminated' with food dye, while the other is uncontaminated. Initially the system is fed with contaminated fluid and the plume is turned on until the system reaches steady state and is uniformly contaminated. Then the source of ambient fluid is switched to the uncontaminated reservoir. Concentration measurements were obtained by dye concentration. The Plexiglas tank was backlit with a fluorescent light source and the experiments were recorded and analysed with the image processing package DigImage. The light intensity at each point in the tank is recorded and correlated to the concentration of contaminant present. Using pre-determined calibration curves of light intensity against concentration, the local concentration of contaminant within the box can be inferred. The vertical concentration profiles are then horizontally averaged across the entire width of the tank, excluding the zone with the plume in order to reduce noise. The standard deviation associated with this averaging process is small (typically less than 5% of the average value), suggesting good accuracy.

5. Experimental results

Figure 8 displays the results from a series of experiments for an interface at $0.25H$, $0.5H$ and $0.75H$. The measured levels of contaminant over time are compared to those predicted by the theoretical models. As can be seen, the qualitative comparison is good. The lower layer seems to be better described by the well-mixed model for the two lower interfaces, although some displacement behaviour is definitely visible,

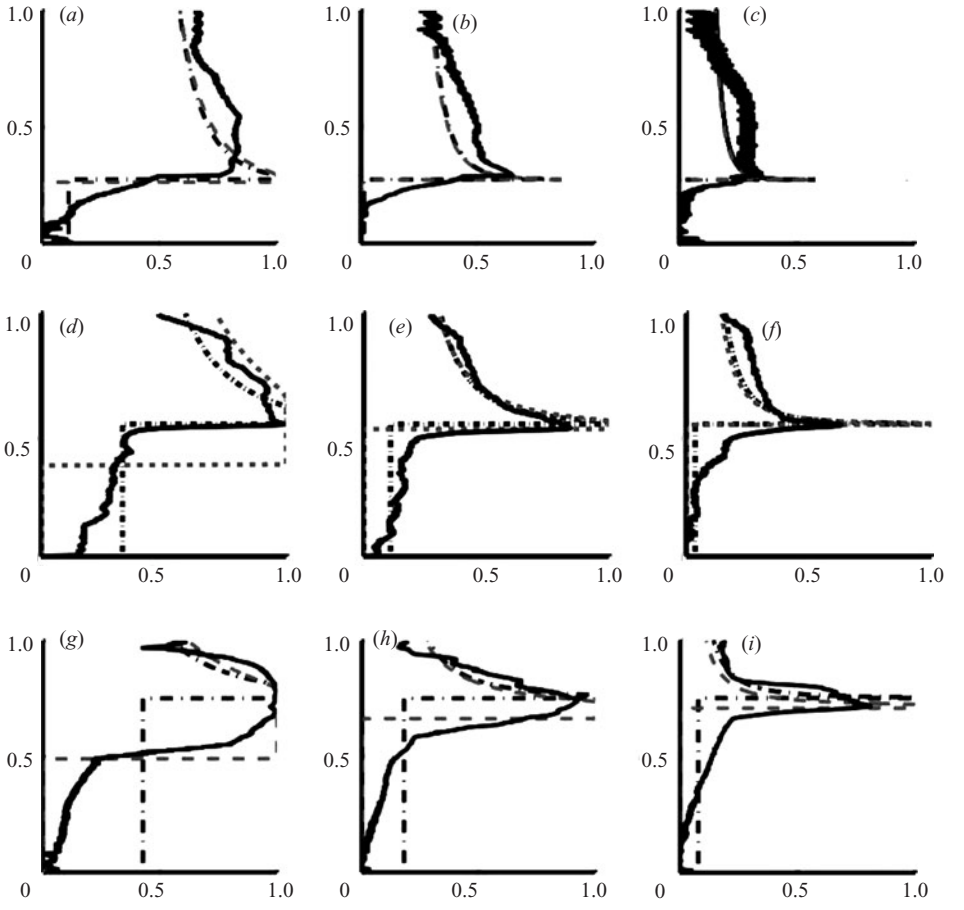

FIGURE 8. Vertical concentration profiles for (*a*)–(*c*) $\zeta_h = 0.25$, (*d*)–(*f*) $\zeta_h = 0.5$ and (*g*)–(*i*) $\zeta_h = 0.75$, at time intervals of 0.6τ, 1.2τ and 1.8τ. Experiments (–), well-mixed lower layer (-·), displaced lower layer (- -).

particularly at early times. The quantitative disagreement can probably be attributed to the fact that the finite area and momentum of the fluid entering through the vents causes some level of mixing, which, as mentioned above, we attempted to minimize by placing the deflecting plates below the inlets. The location of the inlets also plays an important role, because certain parts of the lower layer will become contaminated faster than others and so the plume will not necessarily be exposed to an average amount of contaminant instantly. This is very much an issue for real displacement ventilation systems, where such considerations are important. However, despite these experimental shortcomings we get good quantitative agreement.

One of the most important features present is the peak in concentration of contaminant at the interface level. Quantitatively the agreement is not all that good here and this is probably due to the finite thickness of the interface, which can exchange fluid with the surrounding space, thus losing high-concentration contaminant by entrainment into the plume and replenishing it with lower concentration fluid from the lower and upper layers. However, this concentration peak is clearly observed to be a robust feature of the experiments and marks a significant difference from well-mixed ventilation.

6. Discussion

The present study looks at the transport of a contaminant in a displacement ventilation system with a single source of buoyancy. In order to study this problem the 'step-down' method is used, where the space is initially filled uniformly with contaminant. Then fresh uncontaminated air is introduced into the space through the vent. For a passive contaminant the results are equivalent and exactly opposite to the 'step-up' method, where contaminant enters an initially uncontaminated space.

The analytical solutions indicate that this problem displays some interesting and perhaps unexpected behaviour. The present study illustrates that displacement ventilation may not be better than traditional mixing systems at removing contaminants. Displacement ventilation takes advantage of the natural stratification that will arise in a space, extracting air of the warmest temperature that naturally rises to the top of the room. Nevertheless, the air that is being extracted may not be the most contaminated, since the velocity field for these low-energy systems advects contaminants towards the interface between the lower and upper layers. Thus the contaminant extraction process does not utilize the mechanism that offers displacement ventilation its improved energy efficiency. Instead, the concentration at the outlet vent is relatively insensitive to the ventilation scheme, giving similar overall flushing rates.

In § 3 and § 4 it is observed that the peak level of contaminant for this 'step-down' analysis occurs at the interface between the upper and lower layers. Therefore, depending on the location of this interface, while people sitting down may be in the clean lower layer, someone who stands up may have their head at the peak concentration height. As such, the height of the interface is not only important from a comfort perspective, but also becomes a critical parameter in the design for IAQ. Another issue to consider is the following. In this experiment we have filled the room with contaminant initially and then introduced fresh air through the lower vents. What if the source of contaminant is the ventilation system? This corresponds to the 'step-up' case discussed above. Now the exact opposite situation occurs to that we just described, which means that the highest concentration of contaminant will exist in the 'occupied' lower layer.

There is a simple explanation as to why displacement ventilation does not exhibit the same benefits for removal of contaminants as it does for heat. The efficiency of displacement ventilation at removing heat stems from the fact that warmest air is always extracted from the top room. For a passive contaminant this high-efficiency mechanism does not take place, since the location of maximum contaminant and temperature do not coincide.

Finally, we have compared displacement and mixing systems for the same ventilation flow rate. In practice, displacement ventilation offers two methods of energy savings. Either the incoming air is introduced at a warmer temperature than with a mixing system, thus saving energy on the cooling system, or the incoming flow rate could be reduced, thus saving on fan power. This study suggests that the first option is the more sensible one for IAQ since a lower flow rate will yield an even lower contaminant removal efficiency. It is often also the most sensible from an energy approach, since cooling is typically more expensive than fan power.

It is important to point out that the flow modelled in this paper is forced displacement flow. However, there is no reason to expect the behaviour to be any different for the buoyancy-driven flow such as displacement natural ventilation. The only difference is that in one case the flow is forced through the space and the plume only provides the resulting stratification, while for natural ventilation the buoyancy

provided by the plume leads to a stratification that in turn causes the flow through the system. Once both systems reach steady state they behave in a similar manner, and therefore all the analysis and observations made should hold for both systems.

For the other common case, of an isolated release at a specific location within a space, this model may not be applicable. While it is widely believed that studying the 'step up', 'step down' and isolated-release cases are equivalent (Coffee & Hunt 2005), we believe that displacement ventilation does not dilute the space as effectively as mixing ventilation. Therefore, local concentrations of contaminant should be higher and the efficiency of removal will depend on the location of the source.

REFERENCES

Baines, W. D. & Turner, J. S. 1969 Turbulent buoyant convection from a source in a confined region. *J. Fluid Mech.* **37**, 51–80.

Brohus, H. & Nielsen, P. V. 1996 Personal exposure in displacement ventilated rooms. *Indoor Air* **6**, 157.

Caulfield, C. P. & Woods, A. W. 2002 The mixing in a room by a localized finite-mass-flux source of buoyancy. *J. Fluid Mech.* **471**, 33–50.

Coffey, C. J. & Hunt, G. R. 2007 Ventilation efficiency measures based on heat removal. Part 1. Definitions. *Building Environ.* **42**, 2241–2248.

Cook, M. J., Ji, Y. & Hunt, G. R. 2003 CFD modelling of natural ventilation: Combined wind and buoyancy forces. *Intl J. Ventilation* **1**, 169–180.

Germeles, A. E. 1975 Forced plumes and mixing of liquids in tanks. *J. Fluid Mech.* **71**, 601–623.

He, G., Yang, X. & Srebric, J. 2005 Removal of contaminants released from room surfaces by displacement and mixing ventilation: Modeling and validation. *Indoor Air* **15**, 367–380.

Hunt, G. R., Cooper, P. & Linden, P. F. 2000 Thermal stratification produced by jets and plumes in enclosed spaces. In *Proc. Roomvent 2000: 7th Intl Conf. on Air Distribution in Rooms* (ed. H. B. Awbi), pp. 191–198. Elsevier.

Hunt, G. R. & Kaye, N. B. 2006 Pollutant flushing with natural displacement ventilation. *Building Environ.* **41**, 1190–1197.

Jenkins, P. L., Phillips, T. J., Mulberg, E. J. & Hui, S. P. 1992 Activity patterns of Californians: Use and proximity to indoor pollutant sources. *Atmos. Environ.* A **26**, 2141–2148.

Ji, Y., Cook, M. J. & Hanby, V. 2007 CFD modelling of natural displacement ventilation in an enclosure connected to an atrium. *Building Environ.* **42**, 1158–1172.

Kaye, N. B. & Hunt, G. R. 2007 Heat source modelling and natural ventilation efficiency. *Building Environ.* **72**, 1624–1631.

Kaye, N. B. & Hunt, G. R. 2004 Time-dependent flows in an emptying filling box. *J. Fluid Mech.* **520**, 135–156.

Lin, Y. J. P. & Linden, P. F. 2002 Buoyancy-driven ventilation between two chambers. *J. Fluid Mech.* **463**, 293–312.

Lin, Z., Chow, T. T., Fong, K. F., Tsang, C. F. & Wang, Q. 2005 Comparison of performances of displacement and mixing ventilations. Part II. Indoor air quality. *Intl J. Refrigeration* **28**, 288–305.

Linden, P. F. 1999 The fluid mechanics of natural ventilation. *Annu. Rev. Fluid Mech.* **31**, 201–238.

Linden, P. F., Lane-Serff, G. F. & Smeed, D. A. 1990 Emptying filling boxes: The fluid mechanics of natural ventilation. *J. Fluid Mech.* **212**, 309–335.

Liu, Q & Linden, P. F. 2006 The fluid dynamics of an underfloor air distribution system. *J. Fluid Mech.* **554**, 323–341.

Morton, B. R., Taylor, G. I. & Turner, J. S. 1956 Turbulent gravitational convection from maintained and instantaneous sources. *Proc. R. Soc. Lond.* A **234**, 1–23.

Mundt, E. 2001 Non-buoyant pollutant sources and particles in displacement ventilation. *Building Environ.* **36**, 829–836.

Murakami, S. Ohira, N. & Kato, S. 2000 CFD analysis of a thermal plume and the indoor air flow using k models with buoyancy effects. *Appl. Sci. Res.* **63**, 113–134.

Qiu-Wang, W. & Zhen, Z. 2006 Performance comparison between mixing ventilation and displacement ventilation with and without cooled ceiling. *Engng Comput*. **23**, 218–237.

Sandberg, M. & Etheridge, D. 1996 *Building Ventilation: Theory and Measurement*, 1st edn. Wiley.

Woods, A. W., Caulfield, C. P. & Phillips, J. C. 2003 Blocked natural ventilation: The effect of a source mass flux. *J. Fluid Mech*. **495**, 119–133.

Xing, H., Hatton, A. & Awbi, H. B. 2001 A study of the air quality in the breathing zone in a room with displacement ventilation. *Building Environ*. **36**, 809–820.

Yan, Z. 2007 Large eddy simulations of a turbulent thermal plume. *Heat Mass Transfer* **43**, 503–514.

Zhang, Z. & Chen, Q. 2006 Experimental measurements and numerical simulations of particle transport and distribution in ventilated rooms. *Atmos. Environ*. **40**, 3396–3408.